Predicting Adverse Drug Effects: A Heterogeneous Graph Convolution Network with a Multi-layer Perceptron Approach

Y.-H. Chen[1,2], Y.-T. Shih[3*], C.-S. Chien[3], C.-S. Tsai[4]

1 Dept. of Nephrology, Taichung Tzu Chi Hospital, Taichung, Taiwan
2 School of Medicine, Tzu Chi University, Hualien, Taiwan
3 Dept. of Applied Mathematics, National Chung Hsing University, Taichung, Taiwan
4 Dept. of Management of Information Systems, National Chung Hsing University, Taichung, Taiwan
* yintzer_shih@email.nchu.edu.tw

Abstract

We exploit a heterogeneous graph convolution network (GCN) combined with a multi-layer perceptron (MLP), which is denoted by GCNMLP, to explore potential side effects of drugs. By inferring the relationship among similar drugs, our approach in silico methods shortens the time consumption in uncovering the side effects unobserved in routine drug prescriptions. In addition, it highlights the relevance in exploring the mechanism of well-documented drugs. Our results predict drug side effects with area under precision-recall (AUPR) curve AUPR = 0.941, substantially outperforming the non-negative matrix factorization (NMF) method with AUPR=0.600. Moreover, new side effects are obtained using the GCNMLP.

Author summary

We propose the GCNMLP to study drug side effects. By making better drug side effect prediction our approach improves personalized medicine.

1. Introduction

Adverse drug reaction (ADR) refers to the unexpected, harmful, or uncomfortable reactions of a drug intended to treat disease [1]. The U.S. Food and Drug Administration often removes prescription drugs from the market because of significant side effects [2], which result in enormous health and economic loss [3]. Traditionally, researchers document the side effects of drugs through cell or animal studies [4, 5], as the biochemical interrelationship between the expression and phenotypes of intracellular proteins is used to predict drug side effects at the laboratory development stage. However, these methods are often expensive and resource intensive. Furthermore, many serious side effects are not revealed until much later, highlighting the inadequacy of in vitro and in vivo studies.

Many studies in recent years have demonstrated the ability of machine learning algorithms to predict potential drug side effects [6, 7] by integrating different datasets [8, 9]. Established algorithms have used existing molecular biology databases such as gene expression and drug chemical properties to predict drug performance and possible side effects [10, 11], and the other have exploited internet search-keywords to infer

potential side effects for monitoring drug safety [12]. Natural language processing methodologies have also been applied to extract insights from scientific literatures, electronic medical records, and protein functional databases [13, 14]. Nevertheless, predicting side effects of drugs is still challenging, as drugs may affect multiple proteins, interfering subsequent protein networks [15].

Recently, link prediction methods with a matrix factorization approach have been used to predict drug side effects. Similar to matrix completion, each cell of the matrix represents whether a relationship may exist or not [16]. For example, the matrix low-rank decomposition method based on singular value decomposition (SVD) and non-negative matrix factorization (NMF) are commonly used to solve the problems formulated as link prediction [17, 18]. Tensor factorization, like matrix factorization, can also be used to handle datasets with more than three dimensions to solve the link prediction [19]. The NMF has an advantage over the Bayesian networks since some prior information is required for the latter.

Link prediction can also be solved using the node2vec algorithm. As similar nodes tend to aggregate together, the nodes can be encoded with a biased random walk to represent the features of neighboring nodes. This can further be exploited to predict link existence [20]. This method has also been adopted for drug repositioning from known drug-disease relationships using a heterogeneous network with collaborative filtering [21]. Another study applied a heat diffusion kernel method to predict the relationships among genes, protein function, and disease, achieving an AUC value of 92.3% and reducing the error rate by 52.8% [22]. These studies demonstrate that exploring drugs with similar protein binding properties may pave a new direction for verifying drug reliability and effectiveness.

Network analyses that use link prediction include Random Walk [23] and PageRank [24]. Random walk was applied to predict drug responses in cell lines which classified sensitive and drug resistant cell lines with 85% accuracy [25]. Similarly, graph neural networks have been used in disease prediction and classification [26], in biological information problems [27], in social recommendation systems [28] as well as in knowledge graph applications [29]. Convolutional neural network (CNN) is another widely implemented method for extracting spatial patterns in data or images [30]. Graph convolution network (GCN) is a similar method, but it operates on graphs [31].

In this paper we apply a heterogeneous GCN combined with a multi-layer perceptron (MLP), which is denoted by GCNMLP, to explore potential side effects of drugs. Note that any dataset presented as a network structure can be embedded via GCN for downstream machine learning application. The aggregation of nodes and edges characteristics generates representation learning from the graph, node classification, link prediction, and other tasks [26]. The GCN has been applied to social network research [28], biomedicine networks [32] and knowledge graphs [33]. By inferring the relationship among similar drugs, the GCNMLP shortens the time consumption in uncovering the side effects unobserved in routine drug prescriptions. Our results predict drug side effects with area under precision-recall (AUPR) curve AUPR = 0.941%, which is superior to other well-known methods used in the literatures [25, 39]. In addition, new side effects which were not found in original dataset are obtained using the GCNMLP.

The outline of this paper is as follows. In Section 2 we briefly review some well-known methods which were used to study side effects of drugs. In Section 3 we describe the GCNMLP. Our experiments results are reported in Section 4. In Section 5 we rank the side effects of four drugs inquired from the training model. Finally, some conclusions are given in Section 6.

Dataset

The datasets in this study were downloaded from open resources, where the drug information was obtained from DrugBank Online (see [34]), and the side effects information from the SIDER website [35]. The dataset of

side effects (refer to github.com/yishingene/gcnmlp) contains four columns: 'drugbank_id' is the identification number of the database from the University of Alberta, 'drugbank name' is the drug name, 'umls cui from meddra' is the coded number of the Unified Medical Language System, and 'side_effect_name' is the reported side effect. There are three columns in the file 'semantic_similarity_side_effects_drugs'. The first and the second columns are the pairs of drug names. The third column is the similarity score of drugs from the first and the second columns. The similarity score is calculated through natural language processing from the pretrained model created by NLPLab [36]. The process of combining these datasets is illustrated in Figure 1.

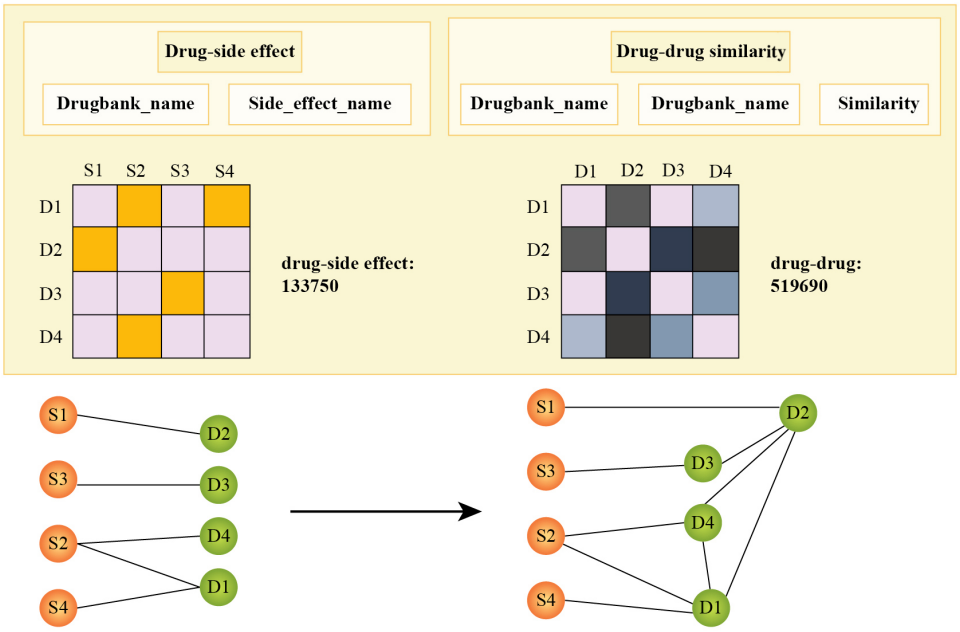

Figure 1. The illustration of the combination of datasets.

2. A brief review of well-known algorithms

For comparison we briefly review some well-known algorithms concerning link prediction.

i. **Non-negative matrix factorization (NMF)**
For convenience we define the set $\mathbb{S} \equiv \mathbb{R}^+ \cup \{0\}$, where $\mathbb{R}^+$ is the set of positive real numbers. Let the relationship between drugs and side effects be described by a bipartite matrix $\mathbf{V} \in \mathbb{S}^{m \times n}$. We factor $\mathbf{V}$ as

$$\mathbf{V} \approx \mathbf{W} \cdot \mathbf{H}, \tag{1}$$

where the matrices $\mathbf{W} = (w_{ij}) \in \mathbb{S}^{m \times k}$ and $\mathbf{H} = (h_{jl}) \in \mathbb{S}^{k \times n}$ are low-rank approximations with dimension $k \ll \min\{m, n\}$, and the recovered elements w_{ij} and h_{jl} in the matrices are the potential links. Note that low-rank matrix factorization could reveal potential links between drugs and side effects [39].

ii. **Non-negative matrix factorization with heat diffusion (NFMHD)**
We apply the heat diffusion equation to the bipartite matrix concerning drug side effects with drug-drug

similarity matrix. Consider an undirected network graph $G = (\mathcal{V}, \mathcal{E}, \mathcal{P})$, where $\mathcal{V} = \{v_1, v_2, \cdots, v_n\}$ is the set of nodes, $\mathcal{E} = \{\overline{v_i v_j}\colon$ for any two connecting nodes v_i and v_j, $1 \le i, j \le n, i \ne j, \}$ the set of all edges, and $\mathcal{P} = \{w_{ij}\}$ is the probability space which is the collection of the link probability w_{ij} for the existence of all edges, $0 \le w_{ij} \le 1$. Let $\mathbf{f}(t)$ be the link vector connecting the nodes v_i and v_j at time t, and $\mathbf{f}(0)$ an initial value at time zero. The discrete approximation for the heat diffusion flow [39, 47] is expressed as

$$\mathbf{f}(t) = e^{\alpha t \mathbf{D}} \mathbf{f}(0), \tag{2}$$

where α is the thermal conductivity coefficient, and $\mathbf{D} = (d_{ij})$ is the diffusion matrix for the node v_j of the undirected graph, which is given by

$$d_{ij} = \begin{cases} -\dfrac{\tau_i}{d_i} \displaystyle\sum_k w_{ik}, & j = i, \\ \dfrac{w_{ji}}{d_j}, & \overline{v_j v_i} \in \mathcal{E}, \\ 0, & \text{otherwise}, \end{cases} \qquad i, j = 1, 2, \cdots, n, \tag{3}$$

for the nodes v_j, where the degrees $d_j \ge 1$, and τ_j is the flag index to the out-line, $0 \le \tau_j \le 1$. Note that the diffusion matrix is derived from the drug-drug similarity matrix.

iii. **Common neighbors** [40]

Let v be a node and Γ_v the set of its neighbors. For any node pair (v_i, v_j) we denote the common neighbors of these two nodes by $\mathrm{CN}(v_i, v_j)$ which is defined as:

$$\mathrm{CN}(v_i, v_j) = |\Gamma_{v_i} \cap \Gamma_{v_j}|,$$

where $|\cdot|$ denotes the cardinal number of a set.

iv. **Jaccard** [41]

The Jaccard of a node pair (v_i, v_j) is defined as

$$\mathrm{Jaccard}(v_i, v_j) = \frac{|\Gamma_{v_i} \cap \Gamma_{v_j}|}{|\Gamma_{v_i} \cup \Gamma_{v_j}|}.$$

v. **Adamic Adar (AA) [42]**

The Adamic Adar computes the probability of two linking nodes v_i and v_j by finding the common neighbors, and calculating the sum of the inverse logarithmic degree of the common neighbors by

$$\mathrm{AA}(v_i, v_j) = \sum_{u \in \Gamma_{v_i} \cap \Gamma_{v_j}} \frac{1}{\log |\Gamma_u|}.$$

vi. **Resource allocation (RA)**

The resource allocation algorithm [43] is designed for predicting the links between two nodes v_i and v_j by measuring the sum of the inverse degree of the common neighbors, and is given by

$$\mathrm{RA}(v_i, v_j) = \sum_{u \in \Gamma_{v_i} \cap \Gamma_{v_j}} \frac{1}{|\Gamma_u|}.$$

vii. **Katz**

The Katz algorithm [44] is a path-based method. The probability of existing links between two nodes v_i and v_j depends on the number of paths between the two nodes, and is given by

$$\mathrm{Katz}(v_i, v_j) = \sum_{l=1}^{\infty} \beta^l \cdot \left[\mathrm{paths}_{v_i, v_j}^{<l>}\right],$$

where β represents the attenuation factor, $\text{paths}_{v_i,v_j}^{<l>}$ is the degree of connection between the nodes v_i and v_j through some walk of length l. Hence the Katz's path is exponentially controlled by the path length, and more weight is required for shorter path.

viii. **Personalized PageRank (PPR)**
The Personalized PageRank $\text{PPR}(v_i, v_j)$ [45,46] calculates either the likelihood of a random walk from the node v_j to the node v_i with a probability ω or a random neighbor with a probability $1-\omega$.

3. The GCNMLP

In this section we describe an end-to-end GCNMLP to predict potential relationships between drugs and side effects. Let $\mathcal{G} = (\mathcal{V}, \mathcal{E}, \mathcal{P})$ be a bipartite graph which represents the network between drugs and side effects, where the sets $\mathcal{V}, \mathcal{E}$ and $\mathcal{P}$ are defined as in Section 2. A homogeneous graph which integrates the similarities between drugs and drugs is attributed to the bipartite network. Let $\mathcal{M} \subset \mathbb{R}^{m\times n}$ be a real matrix which represents a bipartite graph of drugs and side effects, where m is the number of drug effects and n is the number of side effects. Let $p,\ 0 \le p \le m$, be a row index which denotes the drug effect index number, and $q,\ 0 \le q \le n$, a column index representing the side effect index number. The relationship between drugs and side effects is given by $w_{p,q} \in \mathcal{E},\ 0 \le w_{p,q} \le 1$. In addition, $w_{p,q} = 0$ means that there is no connection, and $w_{p,q} = 1$ stands for the connection between drugs and side effects. Otherwise $w_{p,q}$ denotes the unknown predicted value.

The spatial-based method of GCN is similar to that of the convolutional neural network (CNN), where the representations from the neighboring nodes of a given node ν are aggregated and updated. Moreover, it also outputs the representation of the graph required [37]. The GCNMLP is formulated as

$$\mathbf{h}_\nu^k = \sigma(\mathbf{W}_k \sum_{\mu\in\mathcal{N}(\nu)} \frac{\mathbf{h}_\mu^{k-1}}{|\mathcal{N}(\nu)|} + \mathbf{B}_k \mathbf{h}_\nu^{k-1}), \tag{4}$$

where $\mathbf{h}_\nu^k$ represents the feature of the link between the node $\nu \in \mathcal{V}$ and the set of neighbors $\mathcal{N}(\nu)$ with weighting matrices $\mathbf{W}_k$ and $\mathbf{B}_k$, and σ is a differentiable aggregator function in the k-th aggregation step. Equation (4) means that the node ν aggregates representations from each node in the neighborhood $\mathcal{N}(\nu)$ on the previous $(k-1)$-th aggregation step, which is given by $\left\{\mathbf{h}_\mu^{k-1},\ \forall\ \mu \in \mathcal{N}(\nu)\right\}$. When $k = 0$ the representations are just the initial input of the link. Equation (4) can further be generalized as

$$\mathbf{h}_\nu^k = \phi(\text{concat}(\mathbf{h}_\nu^{k-1}, \sum_{\mu\in\mathcal{N}(\nu)} \frac{\mathbf{h}_\mu^{k-1}}{|\mathcal{N}(\nu)|} + \max_{\mu\in\mathcal{N}(\nu)} \mathbf{h}_\nu^{k-1})), \tag{5}$$

where $\phi(\cdot)$ is either a function of a multi-layer perceptron, or dot product of neighboring nodes, or other self-defined functions to represent the link through node features, and 'concat' is the concatenate function where the input features are concatenated. The link probability between two adjacent nodes is predicted as a probability from the node's features. Let $\mathbf{h}_\mu^k$ and $\mathbf{h}_\nu^k$ be the features of two adjacent nodes μ and ν, respectively. We define Φ as a function of the dot product of $\mathbf{h}_\mu^k$ and $\mathbf{h}_\nu^k$ or the multi-layer perceptron. The score of the link between the nodes μ and ν is defined as

$$y_{\mu,\nu} = \Phi(\mathbf{h}_\mu^k, \mathbf{h}_\nu^k).$$

The architecture of the GCNMLP is illustrated in Figure 2.

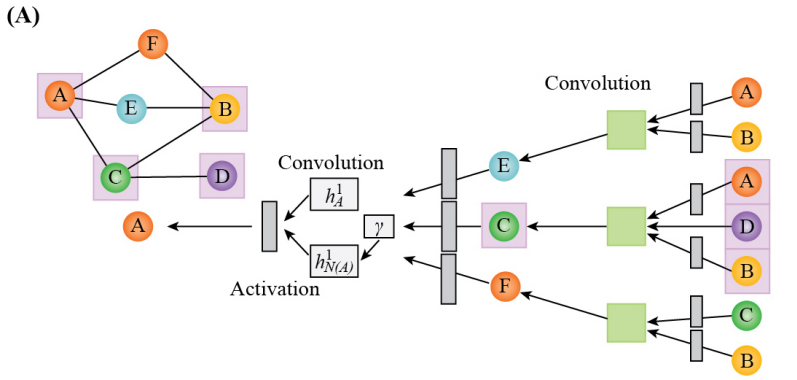

(a) GCN

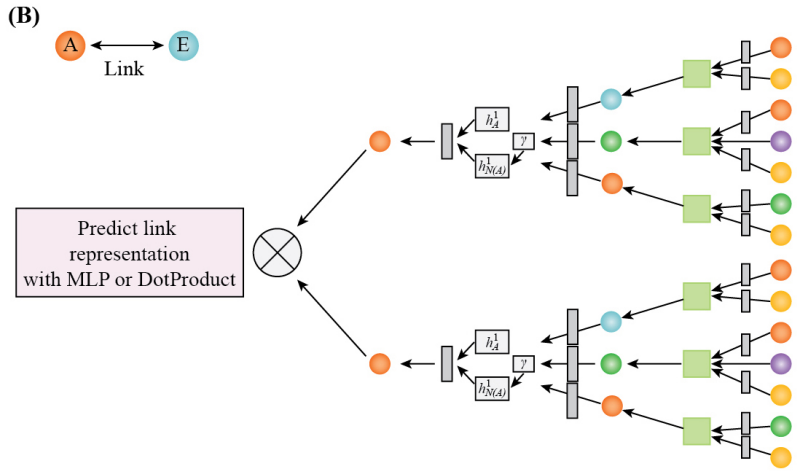

(b) Link prediction

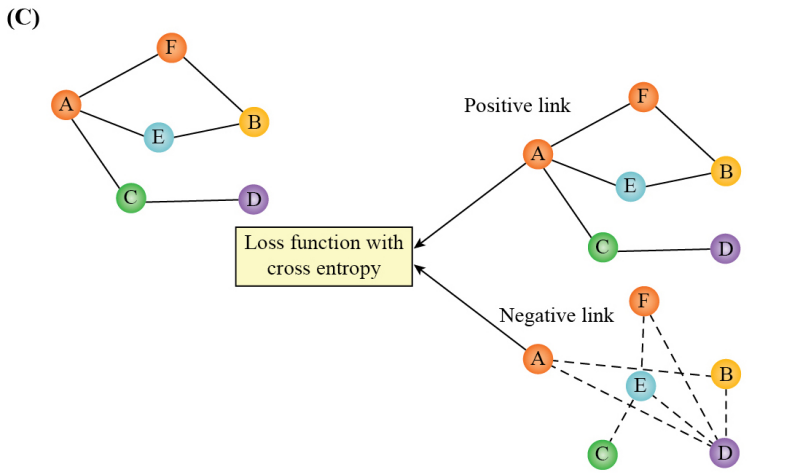

(c) Classification of positive and negative graph

Figure 2. The architecture of the GCNMLP.

4. Experimental Results

In this section, we implemented the GCNMLP for link prediction. The GCN was applied to assess the predictability of drug side effects, and the MLP was exploited to classify the positive and negative graphs. In addition, the dataset was shuffled before being split into 90% for training and 10% for testing. We used the Precision, Recall, F1 score, AUROC, and AUPR as evaluation scales. All experiments were run 10 times including the mean results and the standard deviations.

Comparing different dropout rates in the GCNMLP. The dropout rate is important if we wish to improve the performance of deep learning models. Different dropout rates with 0%, 10%, 30%, 50% were used in our model. We observe from Table 1 that a trend of deteriorating performance occurred on all evaluation scales when the dropout rate was increasing.

Comparing different percentage of the training set in the GCNMLP. Various data sizes of the training set were considered in our experiments. From Table 2 we find that when the size of the training set was decreased from 90% to 80%, the performance on the GCNMLP on all the evaluation scales deteriorates. When the size of the training set was decreased from 80% to 50%, the performance of these two training sets almost makes no difference on all evaluation scales except the AUPR. However, the deviation of the latter is smaller than that of the former.

Comparing different hop numbers in the GCNMLP. We implemented the GCNMLP with different hop numbers. Table 3 shows that the GCNMLP performs best with the hop number being 3. When the hop number $n = 4$ or 5, the performance of the GCNMLP are almost the same on all the evaluation scales except the AUPR. But the deviation of the latter is greater than that of the former.

Comparing the performance of various algorithms. We compared the performance of the GCNMLP to the other methods mentioned in Section 2. Table 4 shows that the GCNMLP performs best among these methods on Recall, F1 score, and AUPR. In addition, the non-negative matrix factorization methods are superior to the heuristic network link-prediction methods on these three items. On the other hand, the NMF outperforms the other methods on AUROC, and the NMFHD is superior to the other methods mentioned above on Precision. Figure 3 displays the AUPR score of various algorithms. Figure 4(a) shows that the NMF performs best on the receiver operating characteristic (ROC) curve among the other methods mentioned above. However, the GCNMLP is quite competitive compared to that of the NMF and NMFHD. Figure 4(b) displays that the GCNMLP is superior to all the other methods on the AUPR. From the results mentioned above it is obvious that the heuristic network link-prediction methods are inferior to the GCNMLP and the non-negative matrix factorization methods on all the items.

Finally, we performed the t-test to find out if there was a significant difference in the 10 fold cross validation results among the GCNMLP and the NMF based methods and the graph-based link prediction methods using a significance level with $\alpha = 0.05$. After the t-test was computed, we computed and compared to the significance level with $\alpha = 0.05$. If the p-value was smaller than α, we rejected the null hypothesis. Table 5 shows the testing results of the p-values.

Discussions

New side effects which were not found in the original dataset could be obtained using the GCNMLP. Here the parameters used were acquired from the dataset after training. We have inquired four drugs from the trained model. The probability scores of the ten highest-ranked side effects of these drugs were calculated and ranked. Tables 6 –7 exemplified the results. Table 6 shows that the side effects, viz, paraesthesia and leukopenia associated with vancomycin, an antibiotic, have high probability which has been reported in [48], and [49, 55], respectively. Besides, the side effect angioedema associated with the drug glimperide is rarely seen, which has been reported in [50] was detected in our experiments. See Table 7. Both Tables 6 and 7 display that most high-ranked side effects are common.

5. Conclusion

We have presented the GCNMLP as an improved method to integrate different datasets and to predict drug side effects. Since the information structure is of network type, such as protein-protein, drug-target, or drug-genome interaction [15, 60], the biomedical data is particularly suitable for the GCNMLP analysis. The GCNMLP outperforms traditional methods, including matrix factorization and similarity-based graph methods. We have demonstrated novel predictions from our model, some of which can be validated in the literatures as shown in Tabs. 6–7. The predicting results show the capabilities of the GCNMLP, which reveals potential link information when combined with heterogenous graphs.

However, the data we chose in our study are only limited to the drug-drug similarity and drug side effect. We may extend the database by including the drug-protein or pharmacogenetics in our study to make a better personalized prediction. Moreover, we may perform the permutation test for the invariant or equivariant nature of graphs [61, 62] in our future study.

In conclusion, our study suggests that the GCNMLP might be used as a model for exploring drug side effects. We can give better personalized medicine using the GCNMLP approach.

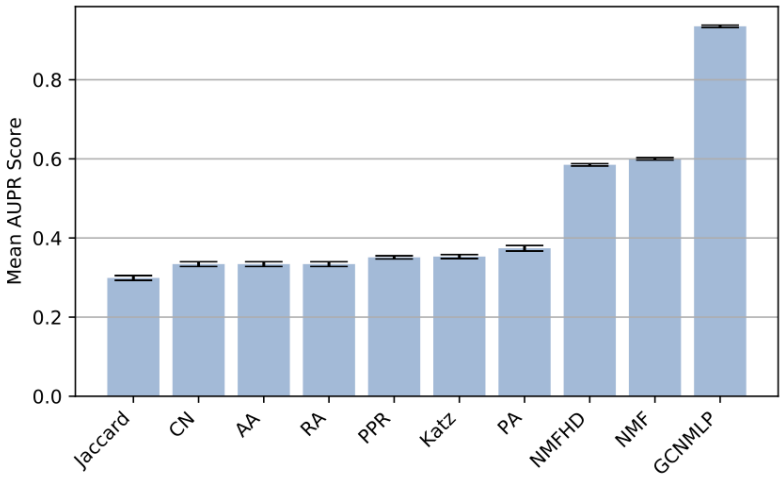

Figure 3. Comparing the performance of various algorithms on AUPR (score).

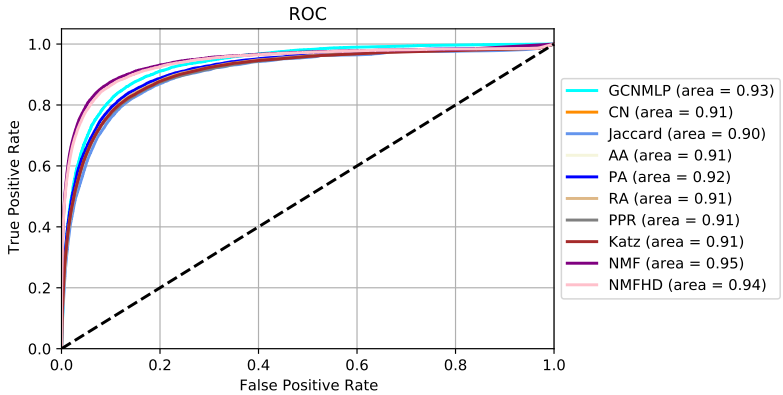

(a)

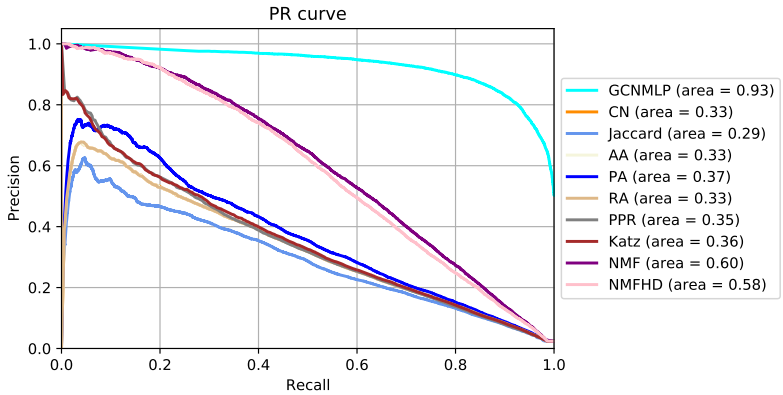

(b)

Figure 4. Comparing the performance of various algorithms on the ROC and PR curves.

References

1. Edwards IR & Aronson JK. Adverse drug reactions: definitions, diagnosis, and management. *Lancet* **356**, 1255–1259 (2000).

2. Friedman MA, Woodcock J, Lumpkin MM, Shuren JE, Hass AE, & Thompson LJ. The safety of newly approved medicines: do recent market removals mean there is a problem? *JAMA* **281**, 1728–1734 (1999).

3. Scheiber J, Chen B, Milik M, Sukuru SC, Bender A, Mikhailov D, Whitebread S, Hamon J, Azzaoui K, Urban L, Glick M, Davies JW, & Jenkins JL. Gaining insight into off-target mediated effects of drug candidates with a comprehensive systems chemical biology analysis. *J. Chem. Inf. Model.* **49**, 308–317 (2009).

4. Bailey J, Thew M & Balls M. An analysis of the use of animal models in predicting human toxicology and drug safety. *Altern. Lab. Anim.* **42**, 181–199 (2014).

5. Gómez-Lechón MJ, Tolosa L, Conde I & Donato MT. Competency of different cell models to predict human hepatotoxic drugs. *Expert Opin. Drug Metab. Toxicol.* **10**, 1553–1568 (2014).

6. Atias N & Sharan R. An algorithmic framework for predicting side effects of drugs. *J. Comput. Biol.* **18**, 207–218 (2011).

7. Zhang W, Zou H, Luo L, Liu Q, Wu W & Xiao W. Predicting potential side effects of drugs by recommender methods and ensemble learning. *Neurocomputing* **173**, 979–987 (2016).

8. Yamanishi Y, Pauwels E & Kotera M. Drug side-effect prediction based on the integration of chemical and biological spaces. *J. Chem. Inf. Model.* **52**, 3284–3292 (2012).

9. Zhang W, Liu W, Chen Y, Wu W, Wang W & Li X. Feature-derived graph regularized matrix factorization for predicting drug side effects. *Neurocomputing* **287**, 154–162 (2018)

10. Muñoz E, Nováček V & Vandenbussche PY. Using Drug Similarities for Discovery of Possible Adverse Reactions. *AMIA Annu. Symp. Proc.* **2016**, 924–933 (2016).

11. Campillos M, Kuhn M, Gavin A-C, Jensen LJ & Bork P. Drug target identification using side-effect similarity. *Science* **321**, 263–266 (2008).

12. White RW, Wang S, Pant A, Harpaz R, Shukla P, Sun W, DuMouchel W & Horvitz E. Early identification of adverse drug reactions from search log data. *J. Biomed. Inform.* **59**, 42–48 (2016).

13. Vilar S, Friedman C & Hripcsak G. Detection of drug–drug interactions through data mining studies using clinical sources, scientific literature and social media. *Brief. Bioinform.* **19**, 863–877 (2017).

14. Vine LD, Zuccon G, Koopman B, Sitbon L & Bruza P. Medical Semantic Similarity with a Neural Language Model. in *Proceedings of the 23rd ACM International Conference on Conference on Information and Knowledge Management* (ACM, 2014) URL `https://doi.org/10.1145/2661829.2661974.`

15. Mizutani S, Pauwels E, Stoven V, Goto S & Yamanishi Y. Relating drug-protein interaction network with drug side effects. *Bioinformatics* **28**(18), i522–i528 (2012).

16. Menon AK & Elkan C. Link Prediction via matrix factorization. in *Machine Learning and Knowledge Discovery in Databases* 437–452 (Springer, Berlin, Heidelberg, 2011).

17. Cai J-F, Candès EJ & Shen Z. A singular value thresholding algorithm for matrix completion. *SIAM J. Optim.* **20**, 1956–1982 (2010).

18. Xu Y, Yin W, Wen Z & Zhang Y. An alternating direction algorithm for matrix completion with nonnegative factors. *Front. Math. China* **7**, 365–384 (2012).

19. Karatzoglou A, Amatriain X, Baltrunas L & Oliver N. Multiverse recommendation: n-dimensional tensor factorization for context-aware collaborative filtering. In: *Proceedings of the Fourth ACM Conference on Recommender Systems*, 79–86 (ACM, 2010).

20. Grover A & Leskovec J. node2vec: Scalable feature learning for networks. *Proceedings of the 22nd ACM SIGKDD International Conference on Knowledge Discovery and Data Mining*, 855–864 (ACM, 2016).

21. Wang H, Gu Q, Wei J, Cao Z & Liu Q. Mining drug-disease relationships as a complement to medical genetics-based drug repositioning: Where a recommendation system meets genome-wide association studies. *Clin. Pharmacol. Ther.* **97**, 451–454 (2015).

22. Nitsch D, Gonçalves JP, Ojeda F, de Moor B & Moreau Y. Candidate gene prioritization by network analysis of differential expression using machine learning approaches. *BMC Bioinformatics* **11**, 460 (2010).

23. Lovász L. Random walks on graphs: a survey, combinatorics, Paul Erdos is eighty *Bolyai Soc. Math. Stud.* **2**, 1–46 (1993).

24. Page L, Brin S, Motwani R & Winograd T. *The pagerank citation ranking: bringing order to the web.* Tech. Rep. Stanford InfoLab. (1999).

25. Stanfield Z, Coşkun M & Koyutürk M. Drug response prediction as a link prediction problem. *Sci. Rep.* **7**, 40321 (2017).

26. Zhou J, Cui G, Hu S, Zhang Z, Yang C, Liu Z, Wang L, Li C & Sun M. Graph neural networks: A review of methods and applications. *AI Open* **1**, 57–81 (2020).

27. Hasibi R & Michoel T. A graph feature auto-encoder for the prediction of unobserved node features on biological networks. *BMC Bioinform.* **22**, 525(2021).

28. Fan W, Ma Y, Li Q, He Y, Zhao E, Tang J & Yin D. Graph neural networks for social recommendation. in *The World Wide Web Conference on - WWW '19* (ACM Press, 2019). URL `https://doi.org/10.1145/3308558.3313488`.

29. Wang X, He X, Cao Y, Liu M & Chua T-S. KGAT: Knowledge Graph Attention Network for Recommendation. in *Proceedings of the 25th ACM SIGKDD International Conference on Knowledge Discovery & Data Mining - KDD '19* (ACM, 2019). URL `https://doi.org/10.1145/3292500.3330989`.

30. Venkatesan R, Li B. Convolutional Neural Networks in Visual Computing: A Concise Guide. Boca Raton, CRC Press; 2017.

31. Zhang S, Tong H, Xu J. et al. Graph convolutional networks: a comprehensive review. Comput Soc Netw **6**, 11 (2019).

32. Nguyen T, et al. GraphDTA: predicting drug-target binding affinity with graph neural networks. *Bioinformatics* **37**, 1140–1147 (2021).

33. Schlichtkrull M, et al. Modeling relational data with graph convolutional networks. in *The Semantic Web* 593–607 (Springer International Publishing, 2018).

34. Wishart DS, et al. DrugBank: a knowledge base for drugs, drug actions and drug targets. *Nucleic Acids Res.* **36**, D901-6 (2008).

35. Kuhn M, Letunic I, Jensen LJ & Bork P. The SIDER database of drugs and side effects. *Nucleic Acids Res.* **44**, D1075-9 (2016).

36. Pyysalo S, Ginter F, Moen H, Salakoski T & Ananiadou S. Distributional semantics resources for biomedical text processing. URL `https://bio.nlplab.org/pdf/pyysalo13literature.pdf`

37. Hamilton WL, Ying R & Leskovec J. Inductive representation learning on large graphs. *arXiv [cs.SI]* (2017).

38. Kingma DP & Ba J. Adam: a method for stochastic optimization. *arXiv [cs.LG]* (2014).

39. Timilsina M, Tandan M, d'Aquin M & Yang H. Discovering links between side effects and drugs using a diffusion based method. *Sci. Rep.* **9**, 10436 (2019).

40. Newman ME. Clustering and preferential attachment in growing networks. *Phys. Review E* **64**, 025102 (2001).

41. Jaccard P. Étude comparative de la distribuition florale dans une portion des Alpes et des Jura. *Bull Soc Vandoise Sci Nat* **37**, 547-579 (1901).

42. Adamic LA & Adar E. Friends and neighbors on the web. *Social Networks* **25**(3), 211–230 (2003).

43. Zhou T, Lu L & Zhang YC. Predicting missing links via local information. *Eur. Phys. J. B* **71**, 623–630 (2009).

44. Katz L. A new status index derived from sociometric analysis. *Psychometrika* **18**, 39–43 (1953).

45. Jeh G & Widom J. Scaling personalized web search. in *Proceedings of the 12th international conference on World Wide Web.* 271-279 (ACM 2003).

46. Fogaras D, Rácz B, Csalogány K, & Sarláos T. Towards scaling fully personalized pagerank: Algorithms, lower bounds, and experiments. Internet Mathematics, **2**(3), 333-358 (2005).

47. Ma H, Yang H, Lyu MR & King I. Mining social networks using heat diffusion processes for marketing candidates selection. in *Proceedings of the 17th ACM Cnference on Information and Knowledge Management* 233–242 (ACM 2008).

48. Cohen LG, Souney PF & Taylor SJ. Paresthesia and back pain in a patient receiving vancomycin during hemodialysis. *Drug Intell. Clin. Pharm.* **22**, 784–785 (1988).

49. Hook EW 3rd & Johnson WD Jr. Vancomycin therapy of bacterial endocarditis. *Am. J. Med.* **65**, 411–415 (1978).

50. Handelsman Y, et al. A randomized, double-blind, non-inferiority trial evaluating the efficacy and safety of omarigliptin, a once-weekly DPP-4 inhibitor, or glimepiride in patients with type 2 diabetes inadequately controlled on metformin monotherapy. *Curr. Med. Res. Opin.* **33**, 1861–1868 (2017).

51. Russell RP. Side effects of calcium channel blockers. *Hypertension* **11**, II42-4 (1988).

52. Hosie J, et al. Comparison of early side effects with amlodipine and nifedipine retard in hypertension. *Cardiology 80 Suppl* **1**, 54–59 (1992).

53. Devasahayam J, Pillai U & Uppaluri C. Acute severe intestinal obstruction secondary to amlodipine toxicity. *QJM* **105**, 467–469 (2012).

54. Periša V, Laslo D, Maričić L & Zibar L. Perindopril/amlodipine-induced thrombotic microangiopathy. *Turk J Emerg Med* 21, 38–41 (2021).

55. Kemeç Z, Kahya Y, Atay A, Demir M & Gürel A Vancomycin dependent pancytopenia- a rare side effect: a case report. *International Journal of Medical Reviews and Case Reports* **3**, 1 (2019)

56. Biller J & Ferro JM. *Neurologic Aspects of Systemic Disease, Part III.* 1211 (Newnes, 2014).

57. Dwivedi K, Saraswat N & Bisht M. Protons confirmation of glimepiride drug using correlation spectroscopy a unique tool of nuclear magnetic resonance spectroscopy. *Math. Sci. Res. J.* **3**, 1–9 (2013).

58. Saito H. Autonomic dysreflexia in a case of radiation myelopathy and cisplatin-induced polyneuropathy. *Spinal Cord Ser Cases* **6**, 71 (2020).

59. Ishihara M, Matsutani N, Ota S & Seki N. A case of posterior reversible encephalopathy syndrome induced by cisplatin/cpemetrexed chemotherapy for lung cancer. *Case Rep. Oncol.* **10**, 235–238 (2017).

60. Turanli B et al. A network-based Cancer drug discovery: from integrated multi-omics approaches to precision medicine. *Curr. Pharm. Des.* **24**, 3778–3790 (2018).

61. Niu C et al. Permutation invariant graph generation via score-based generative modeling. *arXiv [cs.LG]* (2020) URL `https://arxiv.org/abs/2003.00638.`

62. Keriven N & Peyrè G. Universal invariant and equivariant graph neural networks. *Advances in Neural Information Processing Systems.* 32 (NeurIPS, 2019).

Table 1. Comparing different dropout rates in the GCNMLP.

Dropout	Precision	Recall	F1 score	AUROC	AUPR
0%	0.865±0.003	0.865±0.003	0.865±0.003	0.939±0.002	0.941±0.002
10%	0.862±0.003	0.858±0.003	0.858±0.003	0.934±0.002	0.932±0.003
30%	0.857±0.003	0.853±0.003	0.853±0.003	0.926±0.002	0.926±0.002
50%	0.848±0.003	0.843±0.003	0.842±0.003	0.917±0.002	0.918±0.003

Table 2. Comparing different percentage of the training set in the GCNMLP.

Training	Precision	Recall	F1 score	AUROC	AUPR
90%	0.865±0.003	0.865±0.003	0.865±0.003	0.939±0.002	0.941±0.002
80%	0.864±0.004	0.860±0.004	0..860±0.004	0.937±0.002	0.937±0.004
50%	0.864±0000	0.860±0.000	0.860±0.000	0.937±0.000	0.938±0.0000

Table 3. Comparing different hop numbers in the GCNMLP.

hop #	Precision	Recall	F1 score	AUROC	AUPR
$n = 2$	0.863±0.003	0.859±0.003	0.859±0.003	0.935±0.003	0.935±0.003
$n = 3$	0.865±0.003	0.865±0.003	0.865±0.003	0.939±0.002	0.941±0.002
$n = 4$	0.864±0.002	0.864±0.002	0.864±0.002	0.938±0.002	0.939±0.003
$n = 5$	0.864±0.003	0.864±0.003	0.864±0.003	0.938±0.003	0.940±0.004

Table 4. Comparing the performance of various algorithms.

Model	Precision	Recall	F1 score	AUROC	AUPR
GCNMLP	0.865±0.003	**0.865**±0.003	**0.865**±0.003	0.939±0.002	**0.941**±0.002
Non-negative matrix factorization methods					
NMF	0.906±0.003	0.659±0.001	0.726±0.002	0.946±0.001	0.600±0.003
NMFHD	0.930±0.002	0.623±0.002	0.689±0.002	0.943±0.001	0.585±0.003
Heuristic network link-prediction methods					
CN	0.838±0.008	0.528±0.003	0.546±0.005	0.909±0.001	0.334±0.006
Jaccard	0.765±0.012	0.553±0.008	0.584±0.012	0.901±0.001	0.299±0.006
AA	0.840±0.008	0.525±0.003	0.541±0.006	0.909±0.001	0.334±0.006
PA	0.593±0.076	0.501±0.001	0.496±0.002	0.916±0.001	0.374±0.007
RA	0.490±0.006	0.500±0.000	0.494±0.000	0.909±0.001	0.334±0.006
PPR	0.836±0.007	0.542±0.002	0.570±0.003	0.908±0.001	0.351±0.004
Katz	0.778±0.005	0.587±0.004	0.629±0.005	0.909±0.002	0.353±0.005

Table 5. Comparing the p-value of the t-test among the GCNMLP and various algorithms

Model	Precision	Recall	F1 score	AUROC	AUPR
GCNMLP vs CN	5.789e-08	1.991e-33	4.029e-30	1.548e-15	1.684e-33
GCNMLP vs Jaccard	5.449e-15	5.623e-27	2.883e-23	2.406e-17	2.408e-34
GCNMLP vs AA	7.430e-08	5.703e-33	2.019e-29	1.433e-15	1.766e-33
GCNMLP vs PA	3.063e-09	3.129e-36	5.829e-35	2.094e-13	1.270e-32
GCNMLP vs RA	7.124e-31	8.030e-37	7.201e-37	1.423e-15	1.816e-33
GCNMLP vs PPR	7.042e-09	6.455e-35	4.056e-33	3.306e-16	4.561e-38
GCNMLP vs Katz	2.946e-20	8.275e-31	3.736e-29	1.113e-15	9.453e-36
GCNMLP vs NMF	3.459e-19	8.663e-31	2.311e-27	6.940e-10	6.256e-33
GCNMLP vs NMFHD	1.667e-22	2.187e-32	1.928e-29	1.852e-07	1.391e-33

Table 6. New predictions not seen in the present datasets

Vancomycin			Amlodipine		
Side effect	Probabilities	Literatures	Side effect	Probabilities	Literatures
Decreased appetite	1		Diarrhoea	1	[51]
Paraesthesia	1	[48]	Somnolence	1	
Dyspepsia	1		Feeling abnormal	1	
Musculoskeletal discomfort	1		Decreased appetite	0.999	
Anorexia	1		Paraesthesia	0.999	
Hyperhidrosis	1		Dyspepsia	0.999	[52, 53]
Diarrhoea	1		Anorexia	0.999	
Somnolence	1		Musculoskeletal discomfort	0.999	[54]
Feeling abnormal	1		Hyperhidrosis	0.999	
Leukopenia	0.999	[49, 55]	Convulsion	0.999	

Table 7. New predictions not seen in the present datasets, continued

Cisplatin			Glimperide		
Side effect	Probabilities	Literatures	Side effect	Probabilities	Literatures
Diarrhoea	1		Shock	0.99999857	
Somnolence	0.999	[56]	Dry mouth	0.999998	
Decreased appetite	0.999		Leukopenia	0.99999774	[57]
Feeling abnormal	0.999		Confusional state	0.9999976	
Dyspepsia	0.999		Oedema	0.9999975	
Paraesthesia	0.999		Angioedema	0.99999654	[50]
Musculoskeletal discomfort	0.999		Discomfort	0.9999963	
Anorexia	0.999	[58]	Agitation	0.9999962	
Hyperhidrosis	0.999		Vision blurred	0.99999607	
Convulsion	0.999	[59]	Hypertension	0.9999956	